Atomic Layer Deposition of Iridium Oxide Thin Films from $Ir(acac)_3$ and Ozone

Jani Hämäläinen,*,† Marianna Kemell,† Frans Munnik,‡ Ulrich Kreissig,‡ Mikko Ritala,† and Markku Leskelä†

Laboratory of Inorganic Chemistry, Department of Chemistry, P.O. Box 55, FI-00014 University of Helsinki, Finland, and Institute of Ion Beam Physics and Materials Research, Forschungszentrum Dresden−Rossendorf, P.O. Box 510119, D-01314 Dresden, Germany

Received October 20, 2007. Revised Manuscript Received January 16, 2008

Iridium oxide thin films were grown with atomic layer deposition (ALD) from $Ir(acac)_3$ and ozone between 165 and 200 °C. The films were successfully deposited on soda lime glass, silicon substrate with native oxide, and Al_2O_3 adhesion layer. Saturation of the growth rate with respect to both precursors was verified and the film thickness depended linearly on the number of deposition cycles applied. The iridium oxide films had low impurity contents and good adhesion to all tested surfaces. IrO_2 film deposited at 185 °C had homogeneous depth profile and contained 3.5 at % hydrogen and less than 0.5 at % carbon impurities. Resistivities of about 40 nm thick IrO_2 films varied between 170 and 200 $\mu\Omega$ cm. The films deposited above 200 °C were metallic iridium. All the films deposited were crystalline according to X-ray diffraction patterns.

Introduction

Iridium oxide has several applications because of its attractive catalytic, optical, mechanical, electrical, and electrochemical properties. It is a potential material to be used in advanced memory technologies, for example in dynamic random access memories (DRAMs),[1] ferroelectric random access memories (FeRAMs),[2] quantum trap metal-oxide-nitride-oxide-silicon (MONOS) memories[3] and charge-trap flash (CTF) memories.[4] Iridium oxide can be used in organic light-emitting diodes (OLEDs) as interlayers between anodes and organic hole transport layers to enhance the electrical and optical properties[5] and in field emission displays (FEDs) as thermally stable electrodes in metal–insulator–metal field-emission cathodes.[6] Iridium oxide thin films are applicable as pH sensitive microelectrodes for on-chip sensor devices.[7] Additionally, iridium oxide electrodes can be used for measuring H_2O_2.[8] The work function of an iridium oxide thin film is sensitive to NH_3 and NO_2 gases, suggesting that it could be a feasible material for low operation temperature gas sensors.[9,10] As a biocompatible material it is considered for applications in the field of functional electrostimulation, e.g., as implantable neural stimulating electrodes.[11,12] Iridium oxide films have been investigated as catalysts for electrochemical water splitting in polymer electrolyte membrane (PEM) cells for its mechanical stability and corrosion resistance.[13] Iridium oxide is considered a candidate material also for electrochromic applications due to its good optical and electrochemical properties.[14–16]

Iridium oxide thin films can be deposited with several deposition methods such as reactive sputtering[6,9–11,13,17,18] laser ablation,[19] pulsed laser deposition,[18,20,21] sol–gel,[22]

* Corresponding author. E-mail: jani.hamalainen@helsinki.fi. Fax: +358 9 191 50198.
† University of Helsinki.
‡ Forschungszentrum Dresden–Rossendorf.

(1) Nagel, N.; Constrini, G.; Lian, J.; Athavale, S.; Economicos, L.; Baniecki, J.; Wise, M. *Integr. Ferroelectr.* **2001**, *38*, 259.
(2) Kumura, Y.; Ozaki, T.; Kanaya, H.; Hidaka, O.; Shimojo, Y.; Shuto, S.; Yamada, Y.; Tomioka, K.; Yamakawa, K.; Yamazaki, S.; Takashima, D.; Miyakawa, T.; Shiratake, S.; Ohtsuki, S.; Kunishima, I.; Nitayama, A. *Solid-State Electron.* **2006**, *50*, 606.
(3) Lai, C. H.; Wu, C. H.; Chin, A.; Wang, S. J.; McAlister, S. P. *J. Electrochem. Soc.* **2006**, *153*, G738.
(4) Choi, S.; Cha, Y.-K.; Seo, B.-S.; Park, S.; Park, J.-H.; Shin, S.; Seol, K. S.; Park, J.-B.; Jung, Y.-S.; Park, Y.; Park, Y.; Yoo, I.-K.; Choi, S.-H *J. Phys. D: Appl. Phys.* **2007**, *40*, 1426.
(5) Kim, S. Y.; Baik, J. M.; Yu, H. K.; Lee, J.-L. *J. Appl. Phys.* **2005**, *98*, 093707.
(6) Park, T. J.; Jeong, D. S.; Hwang, C. S.; Park, M. S.; Kang, N.-S. *Thin Solid Films* **2005**, *471*, 236.
(7) Ges, I. A.; Ivanov, B. L.; Schaffer, D. K.; Lima, E. A.; Werdich, A. A.; Baudenbacher, F. J. *Biosens. Bioelectron.* **2005**, *21*, 248.
(8) Yang, H.; Kang, S. K.; Choi, C. A.; Kim, H.; Shin, D.-H.; Kim, Y. S.; Kim, Y. T. *Lab Chip* **2004**, *4*, 42.
(9) Karthigeyan, A.; Gupta, R. P.; Scharnagl, K.; Burgmair, M.; Sharma, S. K.; Eisele, I. *Sens. Actuators, B* **2002**, *85*, 145.
(10) Karthigeyan, A.; Gupta, R. P.; Scharnagl, K.; Burgmair, M.; Zimmer, M.; Sulima, T.; Venkataraj, S.; Sharma, S. K.; Eisele, I. *IEEE Sens. J.* **2004**, *4*, 189.
(11) Slavcheva, E.; Vitushinsky, R.; Mokwa, W.; Schnakenberg, U. *J. Electrochem. Soc.* **2004**, *151*, E226.
(12) Hungar, K; Görtz, M.; Slavcheva, E.; Spanier, G.; Weidig, C.; Mokwa, W. *Sens. Actuators, A* **2005**, *123–124*, 172.
(13) Slavcheva, E.; Radev, I.; Bliznakov, S.; Topalov, G.; Andreev, P.; Budevski, E. *Electrochim. Acta* **2007**, *52*, 3889.
(14) Granqvist, C.-G. *Nat. Mater.* **2006**, *5*, 89.
(15) Patil, P. S.; Kawar, R. K.; Sadale, S. B. *Electrochim. Acta* **2005**, *50*, 2527.
(16) Patil, P. S.; Mujawar, S. H.; Sadale, S. B.; Deshmukh, H. P.; Inamdar, A. I. *Mater. Chem. Phys.* **2006**, *99*, 309.
(17) Slavcheva, E.; Schnakenberg, U.; Mokwa, W. *Appl. Surf. Sci.* **2006**, *253*, 1964.
(18) Jia, Q. In *Handbook of Thin Film Materials*; Nalwa, H. S.; Ed.; Academic Press: San Diego, CA, 2002; Vol. 4, pp 677–698.
(19) Wang, C.; Gong, Y.; Shen, Q.; Zhang, L. *Appl. Surf. Sci.* **2006**, *253*, 2911.
(20) Zhang, L. M.; Gong, Y. S.; Wang, C. B.; Shen, Q.; Xia, M. X. *Thin Solid Films* **2006**, *496*, 371.
(21) El Khakani, M. A.; Chaker, M.; Gat, E. *Appl. Phys. Lett.* **1996**, *69*, 2027.

10.1021/cm7030224 CCC: $40.75
Published on Web 03/28/2008

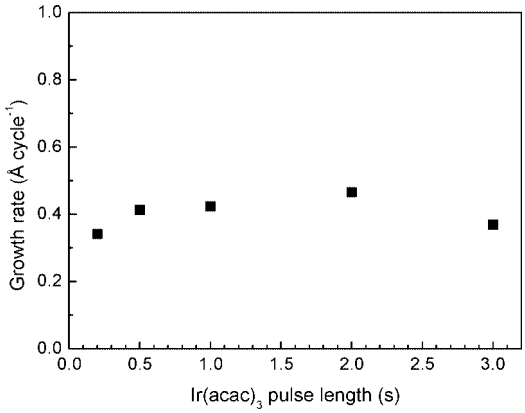

Figure 1. Growth rate of IrO_2 on soda lime glass as a function of $Ir(acac)_3$ pulse length. The ozone pulse length was 1 s. 1000 cycles were applied at 185 °C.

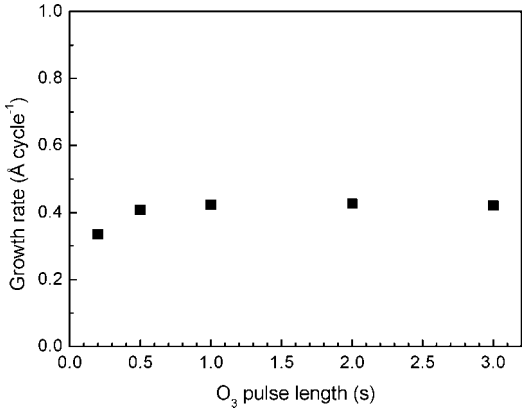

Figure 2. Growth rate of IrO_2 on soda lime glass as a function of ozone pulse length. The $Ir(acac)_3$ pulse length was 1 s. 1000 cycles were applied at 185 °C.

electrochemical deposition,[7,8] spray pyrolysis,[15,16] and chemical vapor deposition.[23,24] Additionally, O_2 annealing[18,25] and plasma treatments[5] of iridium films can be used to produce iridium oxide.

Atomic layer deposition (ALD)[26–29] is considered as one of the most attractive thin film deposition methods in applications where conformality, uniformity, and thickness controllability of the films are crucial. Recently, ALD of noble metals has been extensively studied and metallic films of ruthenium,[30–32] rhodium,[33] palladium,[34,35] iridium,[36–38] and platinum[39,40] have been successfully deposited by

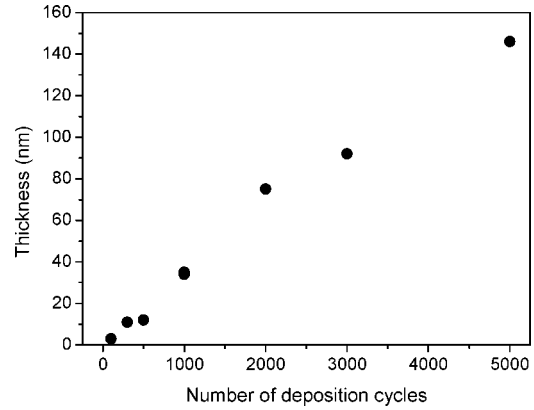

Figure 3. Thickness of IrO_2 on Si(111) substrate as a function of number of deposition cycles. Pulse lengths for both precursors were 1 s and the films were deposited at 185 °C. Thicknesses were determined with EDX.

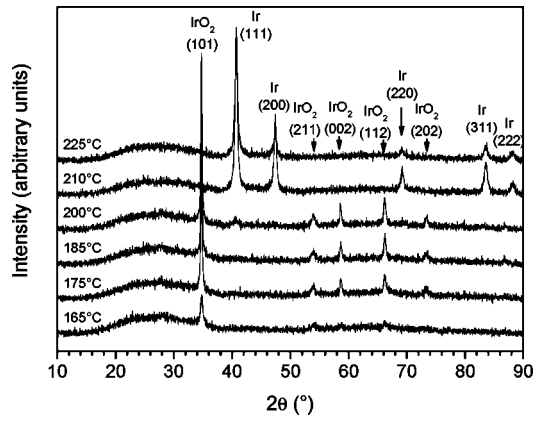

Figure 4. XRD patterns of the films deposited at different temperatures. 2000 cycles were applied in each run. Pulse lengths were 3 s for both precursors. The substrate was soda lime glass with an Al_2O_3 adhesion layer.

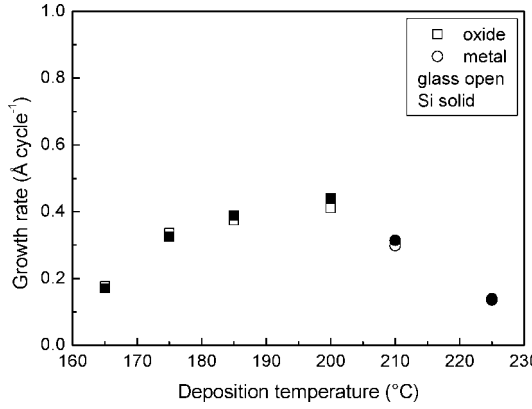

Figure 5. Growth rates of IrO_2 and Ir films on soda lime glass and silicon substrates as a function of deposition temperature. A thin layer of Al_2O_3 was used as an adhesion layer. The pulse lengths were 3 s for both precursors. 2000 cycles were applied in each run.

thermal ALD. Deposition of silver thin films has been introduced by radical enhanced ALD using hydrogen radicals.[41]

Most ALD noble metal processes employ molecular oxygen as a reactive agent. In these processes molecular

(22) Nishio, K.; Tsuchiya, T. *Sol. Energy Mater. Sol. Cells* **2001**, *68*, 279.
(23) Chen, Y.-L.; Hsu, C.-C.; Song, Y.-H.; Chi, Y.; Carty, A. J.; Peng, S.-M.; Lee, G.-H. *Chem. Vap. Deposition* **2006**, *12*, 442.
(24) Chen, R.-S.; Chen, Y.-S.; Huang, Y.-S.; Chen, Y.-L.; Chi, Y.; Liu, C.-S.; Tiong, K.-K.; Carty, A. J. *Chem. Vap. Deposition* **2003**, *9*, 301.
(25) Chalamala, B. R.; Wei, Y.; Reuss, R. H.; Aggarwal, S.; Gnade, B. E.; Ramesh, R.; Bernhard, J. M.; Sosa, E. D.; Golden, D. E. *Appl. Phys. Lett.* **1999**, *74*, 1394.
(26) Ritala, M.; Leskelä, M. In *Handbook of Thin Film Materials*; Nalwa, H. S., Ed.; Academic Press: San Diego, CA, 2001; Vol. 1, pp 103–159.
(27) Puurunen, R. L. *J. Appl. Phys.* **2005**, *97*, 121301.
(28) Elers, K.-E.; Blomberg, T.; Peussa, M.; Aitchison, B.; Haukka, S.; Marcus, S. *Chem. Vap. Deposition* **2006**, *12*, 13.
(29) Leskelä, M.; Aaltonen, T.; Hämäläinen, J.; Niskanen, A.; Ritala, M. *Proc. Electrochem. Soc.* **2005**, *2005–09*, 545.
(30) Aaltonen, T.; Alén, M.; Ritala, M.; Leskelä, M. *Chem. Vap. Deposition* **2003**, *9*, 45.
(31) Aaltonen, T.; Ritala, M.; Arstila, K.; Keinonen, J.; Leskelä, M. *Chem. Vap. Deposition* **2004**, *10*, 215.
(32) Biener, J.; Baumann, T. F.; Wang, Y.; Nelson, E. J.; Kucheyev, S. O.; Hamza, A. V.; Kemell, M.; Ritala, M.; Leskelä, M. *Nanotechnology* **2007**, *18*, 055303.

Table 1. Elemental Compositions of the Iridium Oxide Films Deposited between 165 and 200 °C as Measured with ERDA

dep. temp. (°C)	thickness (nm)	H (at %)	C (at %)	O (at %)	Ir (at %)	O/Ir ratio
165	68	4.50 ± 0.08	0.74 ± 0.11	64.5 ± 0.5	30.3 ± 0.4	$2.08 < X < 2.17$
175	60	3.98 ± 0.09	0.99 ± 0.15	64.2 ± 0.5	30.9 ± 0.4	$2.03 < X < 2.12$
185	68	3.50 ± 0.07	<0.5	64.8 ± 0.5	31.7 ± 0.4	$2.00 < X < 2.09$
200	85	3.21 ± 0.06	<0.5	59.7 ± 0.5	37.1 ± 0.4	$1.57 < X < 1.64$

oxygen is dissociatively chemisorbed on the noble metal surface as atomic oxygen, and some oxygen atoms also diffuse into the subsurface region.[42,43] During the noble metal precursor pulse a reaction takes place between the metal precursor and adsorbed oxygen atoms producing a metallic film. Each process requires a certain threshold temperature to proceed, being governed most likely by the dissociative chemisorption of O_2. Above the threshold temperature, the reaction between the adsorbed oxygen atoms and the metal precursor seems to be so fast that all oxygen becomes consumed and metallic film results instead of an oxide. However, some of the subsurface oxygen atoms may remain if the amount of adsorbed oxygen in the subsurface layer is high, if the noble metal precursor dose is deficient, or if the noble metal precursor pulse time is too short for the reactions to proceed to completion.[42,43] Indeed, using high oxygen partial pressures, ruthenium oxide has been obtained[44,45] and iridium oxide nanodots have been grown by plasma enhanced atomic layer deposition using a mixture of oxygen and hydrogen plasma at 250 °C.[4] On the other hand, as the formation of an oxide film in these processes seems to rely on incomplete reactions, the basic principle of ALD is somewhat violated and accordingly the processes may be less controllable.

Another possible route to the noble metal oxide ALD could be to lower the deposition temperature so that the oxygen atoms deposited in the film would not react with the metal precursor. In this work, we have studied ALD of iridium oxide films using ozone as another precursor. Ozone is more reactive than O_2 and thus can be expected to create adsorbed oxygen atoms at such low temperatures where they would not become consumed in reactions with the metal precursor, thus resulting in an oxide film. By now the use of ozone for noble metal oxide ALD has been reported only in patent literature.[46,47]

Experimental Section

Iridium oxide thin films were deposited in a commercial hot-wall flow-type F-120 ALD reactor (ASM Microchemistry Ltd., Finland) operated under a nitrogen pressure of about 10 mbar. Nitrogen (99.9995%) was produced with a NITROX UHPN 3000 nitrogen generator and used as a carrier and purging gas. The thin films were grown on 5 × 5 cm^2 silicon (111) and soda lime glass substrates. In some cases a thin layer of Al_2O_3 was deposited by

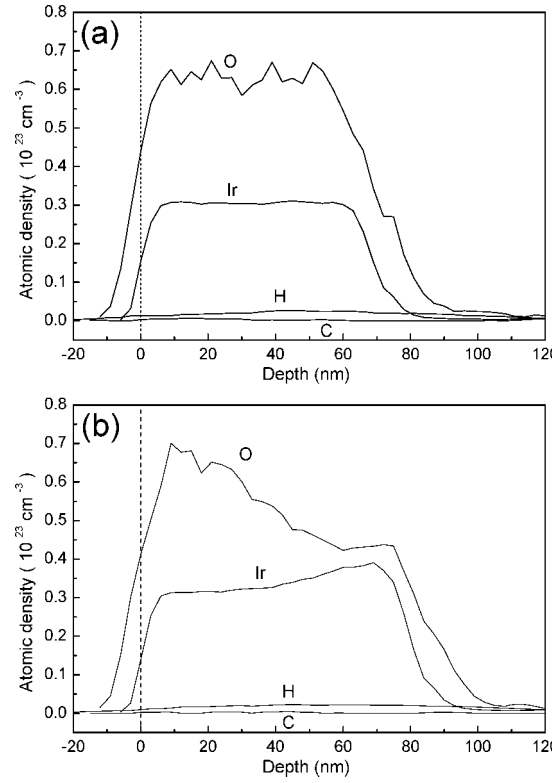

Figure 6. ERDA depth profiles of the iridium oxide films deposited at (a) 185 and (b) 200 °C.

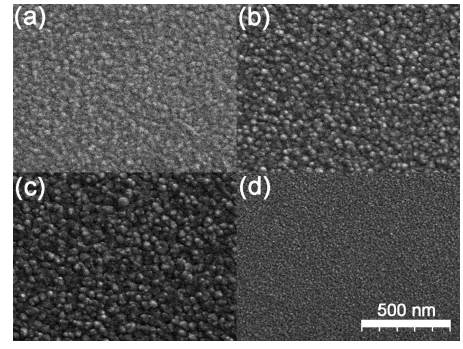

Figure 7. FESEM images of the films deposited at (a) 165, (b) 185, (c) 200, and (d) 225 °C. The film deposited at 225 °C is metallic iridium.

(33) Aaltonen, T.; Ritala, M.; Leskelä, M. *Electrochem. Solid-State Lett.* **2005**, *8*, C99.
(34) Ten Eyck, G. A.; Pimanpang, S.; Bakhru, H.; Lu, T.-M.; Wang, G.-C. *Chem. Vap. Deposition* **2006**, *12*, 290.
(35) Elam, J. W.; Zinovev, A.; Han, C. Y.; Wang, H. H.; Welp, U.; Hryn, J. N.; Pellin, M. J. *Thin Solid Films* **2006**, *515*, 1664.
(36) Aaltonen, T.; Ritala, M.; Sammelselg, V.; Leskelä, M. *J. Electrochem. Soc.* **2004**, *151*, G489.
(37) Färm, E.; Kemell, M.; Ritala, M.; Leskelä, M. *Chem. Vap. Deposition* **2006**, *12*, 415.
(38) Kemell, M.; Pore, V.; Ritala, M.; Leskelä, M. *Chem. Vap. Deposition* **2006**, *12*, 419.
(39) Aaltonen, T.; Ritala, M.; Sajavaara, T.; Keinonen, J.; Leskelä, M. *Chem. Mater.* **2003**, *15*, 1924.
(40) Aaltonen, T.; Ritala, M.; Tung, Y.-L.; Chi, Y.; Arstila, K.; Meinander, K.; Leskelä, M. *J. Mater. Res.* **2004**, *19*, 3353.
(41) Niskanen, A.; Hatanpää, T.; Arstila, K.; Leskelä, M.; Ritala, M. *Chem. Vap. Deposition* **2007**, *13*, 408.
(42) Aaltonen, T.; Rahtu, A.; Ritala, M.; Leskelä, M. *Electrochem. Solid-State Lett.* **2003**, *6*, C130.
(43) Aaltonen, T. Ph. D. thesis, University of Helsinki, Finland, 2005; available from http://ethesis.helsinki.fi/en/.
(44) Kwon, O.-K.; Kim, J.-H.; Park, H.-S.; Kang, S.-W. *J. Electrochem. Soc.* **2004**, *151*, G109.
(45) Kwon, S.-H.; Kwon, O.-K.; Kim, J.-H.; Jeong, S.-J.; Kim, S.-W.; Kang, S.-W. *J. Electrochem. Soc.* **2007**, *154*, H773.

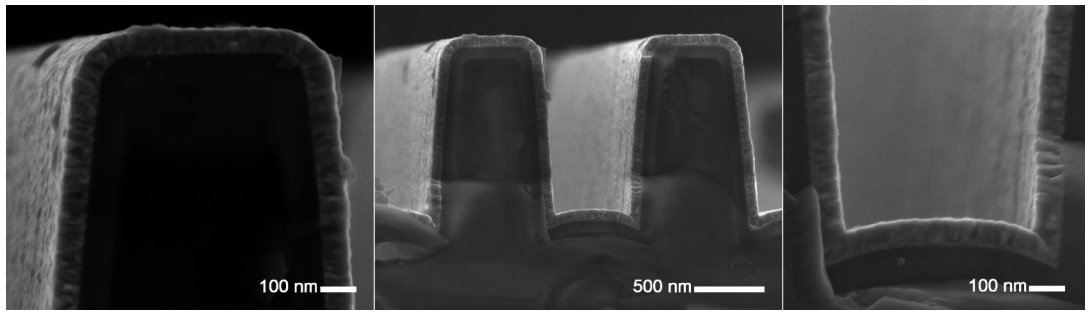

Figure 8. FESEM images of the IrO_2 film deposited at 165 °C on trench patterned Si substrate. 2500 cycles were applied using 5 s pulses and purges for both precursors.

Figure 9. FESEM image of the IrO_2 film deposited onto narrow trench. Growth parameters are the same as in Figure 8.

ALD using trimethylaluminum (TMA) and water prior the iridium oxide. The metal precursor $Ir(acac)_3$ (acac = acetylacetonato) (98%, Strem Chemicals) was sublimed from an open boat held inside the reactor at 155 °C. Ozone was produced with a Wedeco Ozomatic Modular 4 HC Laboratory ozone generator from oxygen (99.999% and 99.9999%, Linde Gas) and pulsed into the reactor through a needle valve and a solenoid valve from the main ozone flow line. The deposition temperature range studied was from 165 to 225 °C. Pulses for both precursors were varied up to 3 s. Each precursor pulse was followed by a 0.5 s nitrogen purge. Onto a trench patterned substrate a film was grown using 5 s pulses and purges.

Crystal structures of the films were identified from X-ray diffraction (XRD) patterns measured with PANanalytical X'Pert Pro and Bruker AXS D8 Advance X-ray diffractometers. Film thicknesses were determined from X-ray reflectivity (XRR) patterns measured with the above-mentioned Bruker diffractometer and from energy-dispersive X-ray spectroscopy (EDX) patterns. The EDX spectra were measured using an Oxford INCA 350 microanalysis system connected to a Hitachi S-4800 field emission scanning electron microscope (FESEM). The spectra were analyzed using a GMR electron probe thin film microanalysis program.[48] Surface morphology of the films was examined by the FESEM. Resistivities of the iridium oxide thin films were calculated from sheet resistances measured with a four-point probe technique and from the film thicknesses. Elemental compositions and depth profiles of the elements were determined with elastic recoil detection analysis (ERDA) using a 35 MeV Cl^{7+} ion beam.[49]

Results and Discussion

Figure 1 shows the growth rate of IrO_2 as a function of the $Ir(acac)_3$ pulse length. A constant growth rate of about 0.4 Å/cycle is achieved with 0.5 s and longer $Ir(acac)_3$ pulse lengths. The effect of ozone pulse length on the growth rate is presented in Figure 2. The growth rate saturates to 0.4 Å/cycle when 0.5 s and longer pulses of ozone are used. Therefore good saturation with respect to both precursors has been obtained as characteristic to ALD. The film thickness seems to depend linearly on the number of the deposition cycles (Figure 3). The rapid nucleation behavior of the iridium oxide film is similar to the metallic iridium deposition from the same iridium precursor and molecular oxygen.[36]

XRD patterns of the films deposited at different temperatures (Figure 4) reveal changes in crystallinity and composition in the temperature range from 165 to 225 °C. The film deposited at 165 °C shows a weak peak corresponding to the (101) reflection of the IrO_2 phase. At the deposition temperature range from 175 to 200 °C, the intensity of the (101) reflection increases and weak reflections of (211), (002), (112) and (202) become visible. A change in the film composition from the iridium oxide to the metallic iridium is apparent between 200 and 210 °C. The XRD patterns of the films deposited at 210 and 225 °C are similar to the diffraction patterns of the metallic iridium films obtained by the process using $Ir(acac)_3$ and molecular oxygen as precursors.[36]

Growth rates of the films deposited between 165 and 225 °C (Figure 5) show that IrO_2 growth rate increases with increasing deposition temperature up to 0.4 Å/cycle at 200 °C. The sublimation temperature of the iridium precursor, 155 °C, determined the lowest deposition temperature studied (165 °C) at which the growth rate was about 0.2 Å/cycle. Growth rates of the metallic iridium films seem to decrease from 0.3 (210 °C) to about 0.15 Å/cycle at 225 °C. This is in good agreement with the process using molecular oxygen as a reactant where no film growth took place at 200 °C, and at 225 °C the growth rate of the Ir film was approximately 0.2 Å/cycle.[36]

Elemental compositions of the films showing IrO_2 in XRD are presented in Table 1. The analyzed films were deposited on an Al_2O_3 adhesion layer on top of Si substrates. The O/Ir ratio of the films decreases from slightly oxygen rich 2.1 to oxygen deficient 1.6 as the deposition temperature increases from 165 to 200 °C. The onset temperature of oxygen deficiency, 200 °C, agrees with the appearance of the first weak XRD reflections of metallic Ir (Figure 4). In the iridium oxide film deposited at 185 °C the O/Ir ratio is closest to 2 indicating stoichiometric IrO_2. Hydrogen impurity content in the film deposited at 185 °C is 3.5 at %, whereas carbon

(46) Marsh, E. P.; Uhlenbrock, S. U.S. Patent 6 881 260, 2005.
(47) Hämäläinen, J.; Ritala, M.; Leskelä, M. U.S. Pat. Appl. Publ. US 2007/0014919, 2007.
(48) Waldo, R. A. *Microbeam Anal.* **1988**, *23*, 310.
(49) Kreissig, U.; Grigull, S.; Lange, K.; Nitzsche, P.; Schmidt, B. *Nucl. Instrum. Methods Phys. Res., Sect. B* **1998**, *136–138*, 674.

content falls below the detection limit of 0.5 at % showing relatively good film purity given that the growth temperature is quite low for thermal ALD oxide deposition. As expected, the hydrogen impurity content in iridium oxide films decreases as the deposition temperature is increased. The detection limit for carbon is relatively high due to the increased background from chloride ions scattered on iridium and from iridium recoil ions. The statistical uncertainty for oxygen is much larger than for iridium, which is reflected in the fluctuations of the respective ERDA profiles (Figure 6). The depth profiles are convoluted with the system resolution and physical effects like straggling. The Y-axis represents the actual quantity of each element directly obtained from the measurements. The X-axis (depth in nm) is obtained using an estimated density and the absolute value should be taken with caution. However, the depths seem to correspond quite well with the thicknesses calculated from EDX data.

The iridium oxide film deposited at 200 °C (Figure 6b) shows a gradual change in composition as the function of the film depth, whereas the film deposited at 185 °C is homogeneous (Figure 6a). In the film deposited at 200 °C the O to Ir ratio is around 2 at the film surface and decreases to almost 1 at the interface. The change in composition is related to the partial reduction of the film (Figure 4). The bump in the oxygen profile at the interface between the film and the substrate in Figure 6a is due to the Al_2O_3 adhesion layer and native SiO_2 layer.

Resistivities of about 40 nm thick iridium oxide films grown on soda lime glass at 185 °C varied between 170 and 200 $\mu\Omega$ cm, whereas the reported values for the [001] and [011] oriented IrO_2 single crystals are 49.1 $\pm$ 0.5 $\mu\Omega$ cm and 34.9 $\pm$ 1.0 $\mu\Omega$ cm, respectively.[50] For IrO_2 thin films deposited by cold-wall chemical vapor deposition, resistivity values of 80 $\pm$ 18 $\mu\Omega$ cm have been reported.[24] Resistivities of 67 $\pm$ 3 and 60 $\pm$ 3 $\mu\Omega$ cm have been obtained by pulsed laser deposition at 250 °C[20] and laser ablation at 300 °C,[19] respectively. In another article,[21] resistivities of the pulsed laser deposited films decreased by about one order of magnitude from substrate temperature of 300 to 400 °C and stabilized around a mean value of about 42 $\mu\Omega$ cm. The authors suggested that as the substrate temperature is increased, the IrO_2 grain size increases and this leads to less grain boundaries, thus decreasing the resistivity. In comparison, the resistivities of about 70 nm thick Ir films grown by ALD are below 12 $\mu\Omega$cm.[36]

Figure 7 shows FESEM images of iridium oxide films grown at 165, 185, and 200 °C. The respective film thicknesses are 68, 68 and 85 nm. The iridium oxide films become more textured as the grain size increases with increasing deposition temperature. For the film deposited at 185 °C, the largest grains are approximately 50 nm in diameter. The 24 nm thick iridium film (Figure 7d) has considerably smoother appearance than the thicker iridium oxide films. Good conformality was verified by growing IrO_2 on trench-structured Si substrate (Figure 8). In Figure 9, the diameter of the trench is smaller and the film has almost filled the whole trench. The iridium oxide films grown on soda lime glass, silicon substrate with native oxide and Al_2O_3 adhesion layer all passed the common tape test regardless of the deposition temperature, indicating good adhesion.

In conclusion, thermal ALD has been employed for iridium oxide thin film deposition between 165 and 200 °C using $Ir(acac)_3$ and ozone as precursors. At higher deposition temperatures, the films became metallic. Good saturation with respect to both precursors was achieved and the film thickness depended linearly on the number of deposition cycles applied. The films had almost stoichiometric composition because of the crystalline IrO_2 phase and the XRD reflections of IrO_2 intensified with increasing deposition temperature. However, at the deposition temperature of 200 °C the depth profile of the film showed a gradual increase in oxygen deficiency near the interface between the film and the substrate. The impurity contents of the films were rather low. The resistivities of the films were considerably higher than the reported values of IrO_2 films deposited with physical and chemical vapor deposition methods. Adhesion of the deposited IrO_2 films was good on all tested surfaces.

Acknowledgment. This work was supported in part by the Finnish Funding Agency for Technology and Innovation (Tekes) and ASM Microchemistry.

CM7030224

(50) Ryden, W. D.; Lawson, A. W.; Sartain, C. C. *Phys. Rev. B* **1970**, *1*, 1494.